International Journal of Mechanical, Industrial and Aerospace Sciences
ISSN: 2517-9950
Vol:8, No:8, 2014

Numerical Simulation of Flow Past an Infinite Row of Equispaced Square Cylinders Using the Multi-Relaxation-Time Lattice Boltzmann Method

S. Ul. Islam, H. Rahman, W. S. Abbasi, N. Rathore

Abstract**—**In this research numerical simulations are performed, using the multi-relaxation-time lattice Boltzmann method, in the range $3 \leq \beta = w[d] \leq 30$ at $Re = 100$, 200 and 300, where β the blockage ratio, w is the equispaced distance between centers of cylinders, d is the diameter of the cylinder and Re is the Reynolds number, respectively. Special attention is paid to the effect of the equispaced distance between centers of cylinders. Visualization of the vorticity contour visualization are presented for some simulation showing the flow dynamics and patterns for blockage effect. Results show that the drag and mean drag coefficients, and Strouhal number, in general, decrease with the increase of β for fixed Re. It is found that the decreasing rate of drag and mean drag coefficients and Strouhal number is more distinct in the range $3 \leq \beta \leq 15$. We found that when $\beta > 15$, the blockage effect almost diminishes. Our results further indicate that the drag and mean drag coefficients, peak value of the lift coefficient, root-mean-square value of the lift and drag coefficients and the ratio between lift and drag coefficients decrease with the increase of Re. The results indicate that symmetry boundary condition have more blockage effect as compared to periodic boundary condition.

Keywords**—**Blockage ratio, Multi-relaxation-time lattice Boltzmann method, Square cylinder, Vortex formation.

I. Introduction

AN infinite row of cylinders is the extreme of a single cylinder case, and the results are expected to be of fundamental values. Flow around cylinders is of practical importance in many fields of engineering and science. The flow past a row of cylinders is of significance in situations such as flow around closely spaced electrical power poles, multi-slotted airfoils, and turning vanes in duct elbows [1]. In spite of single square cylinder studies, the investigations of cross-flow around square cylinder with equispaced distances need more attention because of the numerous parameters such as physical quantities, Reynolds number (Re), and limitations of the different numerical methods could affect the flow patterns. The present study proposes to examine in detail blockage effect (β) of rectangular cylinders is a fundamental element in practical problems such as closely spaced electrical power poles and multi-slotted airfoils.

Shams-Ul-Islam is with the Mathematics Department, COMSATS Institute of Information Technology Islamabad, 44000, Pakistan (corresponding author, Phone: 0092-3139840066; e-mail: islam_shams@comsats.edu.pk).

Hamid Rahman and Waqas Sarwar Abbasi are with the Mathematics Department, COMSATS Institute of Information Technology Islamabad, 44000, Pakistan (e-mail: hamid_icp@yahoo.com, waqas-555@hotmail.com).

The flow around a single square cylinder was studied experimentally and numerically by several researchers. There is not enough experimental data at low Reynolds number in open literature. The difference may be due to two reasons. One is due to the existence of vibrations in real experiments; the second is due to the difficulties related with experimental measurement. Okajima [2] has conducted a wide-ranging experimental study of rectangular bluff body over a wide range of Reynolds numbers between 70 and 2×10^4. He found that the Strouhal number (St) of a square cylinder varies a little with a Reynolds number. Davis et al. [3] carried out a numerical simulation study of the flow past rectangular cylinders and compared the numerical results with Okajima [2] experimental results over a Reynolds number range of 100-2000. Their results show that an increase in blockage increases the drag coefficient (Cd) and the St. Franke et al. [4] carried out numerical simulations of the laminar vortex shedding past a square cylinder of $Re \leq 300$. Sohankar et al. [5] carried out numerical simulations for unsteady two-dimensional flow around a square cylinder, for Re between 45 and 250 using quite different numerical methods. They also investigated the influence of the location of the inflow, outflow and side walls (blockage), respectively at $Re = 100$ Sohankar et al. [6], employed an implicit fractional step method finite-volume code to simulate three-dimensional flow around a square cylinder for Re from 150 to 500. Their results show the transition from two-dimensional to three-dimensional between Reynolds numbers 150 and 200. Saha et al. [7] carried out numerical simulations for flow past a square cylinder at various Re from 40 to 600. They examined the chaotic behavior through the calculation of Lyapunov exponent and fractal dimension. The motivation for the preset study has been taken into account after studying the following available literature.

Ingham et al. [8] examined the flow past a row of normal flat plates using quite different numerical methods. Fornberg [9] proposed quite different numerical methods to examine the physical quantities such as Cd for the flow past a row of circular cylinders at large Re. He examined the transition from small blockage ratio $\beta = w[R]$ (where R is the radius of the circular cylinder) to high β and find the critical range $\beta \approx 8$. Ingham and Yan [10] studied theoretically and numerically the flow past a row of flat plates and square cylinders. In case of square cylinders they employed the central-difference scheme at a fairly low Re. Natarajan et al. [11] considered the same problem of [8] for flow past a row of flat plates at large Re

using Galerkin finite element discretization for the Navier-Stokes (NS) equations in the form of vorticity formulation. They covered the β within the range $5 \leq \beta \leq 25$. They examined that the typical practical situation is almost the same to [9] for the flow past a row of circular cylinders. Kumar et al. [12] studied flow around a row of square cylinder using the lattice Boltzmann method. Their simulations were carried out for two-dimensional flows at a fairly low Reynolds number (Re = 80) and placed flow around a row of nine square cylinders normal to the oncoming flow. Recently, we studied flow past a row of circular cylinders using the lattice Boltzmann method [13].

The rest of this paper is organized as follows: A more detail description of the problem will first be given in Section II. Next, in Section III we will briefly describe the initial and boundary conditions. In Section IV we present extensive numerical results for variety of different β in the Re range between 100 and 300 including comparison with open literature data. In this section we present our numerical results for physical quantities as functions of blockage ratios and Reynolds numbers. Finally, in Section V we draw some conclusions.

II. Problem Description

We consider the flow past an infinite row of equispaced square cylinders as illustrated in Fig. 1. The inflow and outflow boundaries are situated to allow at least 12 diameters between the inflow boundary and the cylinder and 48 diameters between the outflow boundary and the cylinder. In this study, the uniform inflow velocity *Ui* is fixed to be 0.04385686 for all Reynolds numbers. The single-relaxation-time τ is defined by $\tau = U_i d / C_s^2 \Delta t Re + 0.5$, where *C*s is the speed of sound equal to1/sqrt(3), d is the diameter of the cylinder and Δt is the time step. The values of the single-relaxation-time are 0.5263, 0.5131, and 0.5087 for Reynolds numbers 100, 200, and 300, respectively. The computational domain in the streamwise direction is fixed to be *60d and* the lateral direction varies from 3*d* to30*d*.

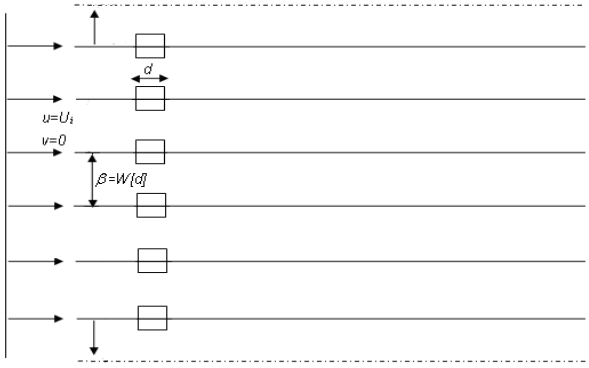

Fig. 1 Schematic flow configuration

The detail about multi-relaxation-time lattice Boltzmann method, important physical parameters, effect of computational domain, grid independence and code validation are given in [14], [15].

III. Initial and Boundary Conditions

The following procedure is incorporated as an initial condition:

$$u = v = 0; \tag{1}$$

and

$$p = p_0 \tag{2}$$

Uniform flow is incorporated using the equilibrium particle distribution function at the inlet in the following way:

$$f_i = f_i^{(0)}(U_i) \tag{3}$$

where f_i and $f_i^{(0)}$ are the particle distribution function and equilibrium distribution function, respectively.

Symmetric boundary condition is adopted to examine the blockage effect. (Comparison between the periodic boundary condition and the symmetry boundary condition is shown later in Section IV) The boundary conditions at j = 1 for the particle distribution function is given by the following way:

$$\begin{aligned} &f_0^{(i,1)} = f_0^{(i,3)}, f_1^{(i,1)} = f_1^{(i,3)}, f_2^{(i,1)} = f_4^{(i,3)} \\ &f_3^{(i,1)} = f_3^{(i,3)}, f_4^{(i,1)} = f_2^{(i,3)}, f_5^{(i,1)} = f_8^{(i,3)}, \\ &f_6^{(i,1)} = f_7^{(i,3)}, f_7^{(i,1)} = f_6^{(i,3)}, f_8^{(i,1)} = f_5^{(i,3)} \end{aligned} \tag{4}$$

Similar condition adopted for $j = NY$.

The surface of the cylinder was defined with a no slip wall boundary condition and this is realized with a bounce-back boundary treatment. No-slip condition ensures that the fluid will have zero velocity relative to the boundary.

The momentum exchange method proposed by [16] was used in the present work for simulating flow around square cylinder.

IV. Results and Discussions

Numerical calculations were carried out for flow past a row of equispaced square cylinders to study blockage effect. Firstly, we will discuss the effect of blockage in this section. Vortex shedding is a key characteristic of interest here. The effects of β in the form of vorticity contour lines behind the cylinder are described in Figs. 2-4 at Re = 100, 200 and 300. In these figures the negative vorticity (clockwise vortex) is shown by dashed lines and the positive vorticity (anticlockwise vortex) by solid lines. It may be important to state here that during the process of numerical simulations for blockage ratios effect flow evolution up to some extent, however, for the sake of brevity only a few selected representative cases will be discussed here.

In Fig. 2 (a), it can be seen that large value of the vortex-shedding Strouhal number shows the very dense arrangement of vortices. The results show that when there is not enough

space in the lateral direction the vortices are cracked down and seem to disappear in the far wake region. The negative vortex is generated at the top corner of the cylinder and more behind the cylinder as it grows and is rolling up on the upper side of the cylinder (Fig. 2 (b)). The negative-signed vortices generated at the front upper grow and then push down the positive-signed vortices from the lower side as shown in Figs. 2 (c), (d).

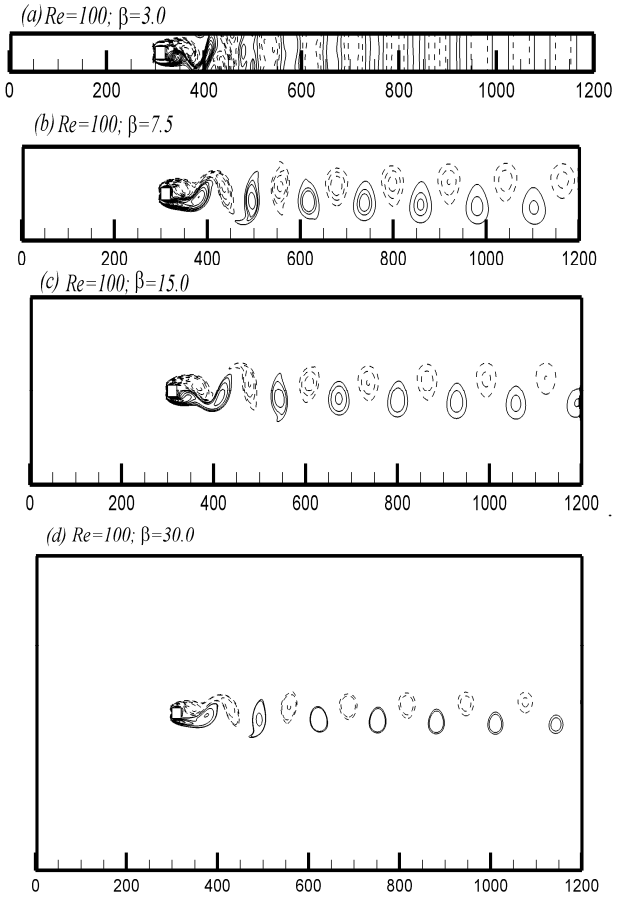

Fig. 2 Vorticity contour lines for different blockage ratios at Re = 100

The results show again that when there is not enough space in the lateral direction the vortices are cracked down and seem to disappear in the far wake region (see Fig. 3 (a)). The alternating vortices almost with the same strength and size are shed from the upper and lower sides of the cylinder for Re = 200. While at β = 15 and Re = 200 (Fig. 3 (b)), from the upper side of the wake the positive vortex draws the shear layer of opposite sign and cuts the supply of vorticity to the positive vortex at the wake centerline. The results show that the distance between consecutive vortices remains almost constant (Fig. 3 (c)). The negative-signed vortices generated at the front upper grow and then push down the positive-signed vortices from the lower side as shown in Fig. 3 (c). The vortices are made stronger and smaller in size with the higher β (Fig. 3 (d)).

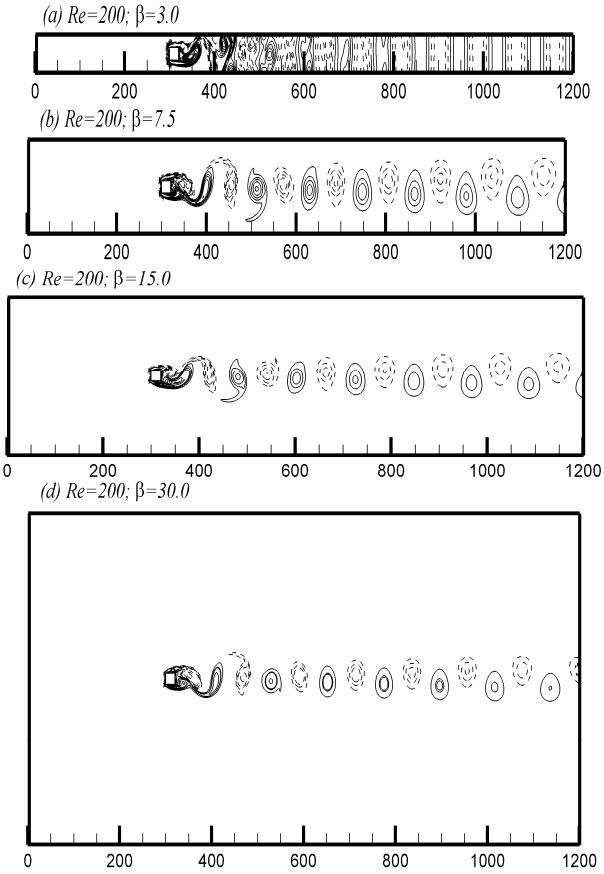

Fig. 3 Vorticity contour lines for different blockage ratios at Re = 200

In Fig. 4 (a) it can be seen again that the vortices are cracked down and seem to disappear in the far wake region. This is due to not enough space in the lateral direction. The results show that the distance between consecutive vortices remains almost constant (Figs. 4 (b), (c)). The vortices are made stronger and smaller in size with the higher β (Fig. 4 (d)).

The results further show that the vortices develop in the near wake undergo successive interactions among themselves when β > 3. It is further noticed, that the width and size of the vortices becomes smaller and stronger when the Re increase from 100 to 300 (Figs. 3 (d) and 4 (d)). These width and size changes between the vortices are due to the fact that the vortices are shed at a higher frequency in these cases.

Some of the important variables of engineering interest for flow past cylinder with vortex shedding are the Cd, $<Cd>$, Cl, root-mean-square value of the lift coefficient ($Clrms$), root-mean-square value of the drag coefficient ($Cdrms$), ratio between the value of lift and drag coefficients (Cl/Cd), and St. Figs. 5-8 show the variation of all such physical quantities with varying β for fixed Re.

The present results show that the Cd, and $<Cd>$, in general, decrease with the increase of β (Figs. 5 (a), (b)). This observation is consistent to the finding of Fornberg [9] for flow past a row of circular cylinders. It is found that the

decreasing rate of *Cd* and <*Cd*> is more distinct in the range 3 ≤ β ≤ 10. On the other hand, the reduction of these physical quantities becomes slight and especially for the last two blockage ratios β = 25 and 30 the reduction becomes insignificant. It is noted that *Cd*, and <*Cd*> reach their maximum values at the blockage ratio (β = 30) (see Figs. 5 (a), (b)). For the blockage ratio β = 3 case, the maximum values for *Cd*, and <*Cd*> given by 2.946 and 2.9161 for Reynolds number 100, 3.046 and 2.9157 for Reynolds number 200, and 3.246 and 3.0404 for Reynolds number 300, respectively.

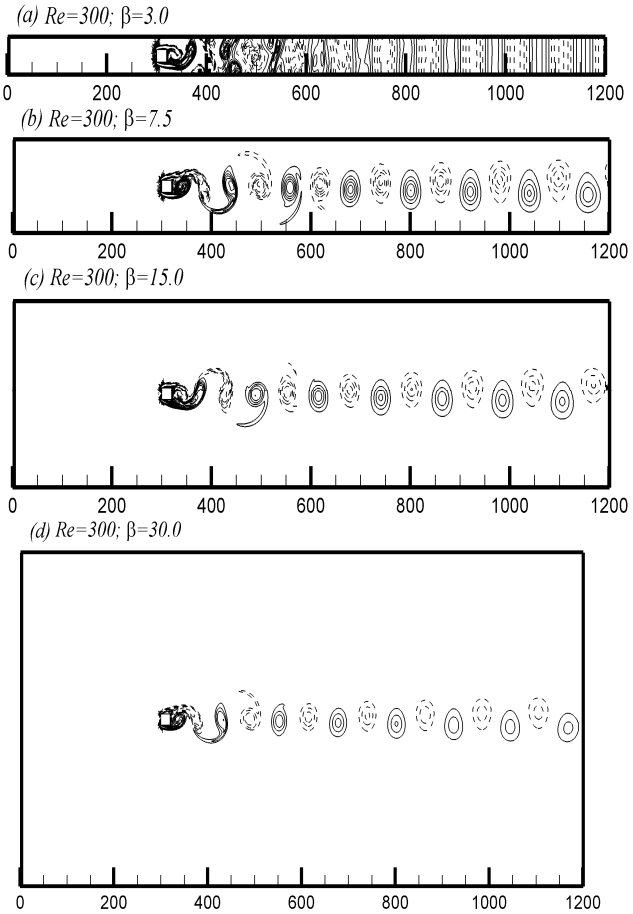

Fig. 4 Vorticity contour lines for different blockage ratios at *Re* = 300

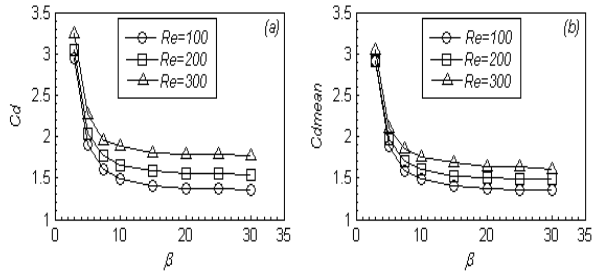

Fig. 5 (a) Drag coefficient (b) mean drag coefficient as a function of the blockage ratios for flow past the cylinder for fixed Reynolds number

The present results further show that the *St*, in general, decrease with the increase of β (Fig. 6 (a)). Fig. 6 (b), shows that for the computed range of β, *Cl* initially increases and then almost remains constant in some cases of β while for some cases it shows a slight decrease for *Re* = 100. In case of *Re* = 200 peak value of lift coefficient initially increases and then shows a slight decrease and then almost remains constant. On the other hand, the *Cl* initially increases and then it shows a slight decrease and increase for some cases of β at *Re* = 300. The increase in *St* as the β is brought closer from a distance of 3*d* to 30*d* is about 39.6% at *Re* = 100, about 36.9% at *Re* = 200 and is about 34.3% at *Re* = 300, respectively. On the other hand, *Cl* appears to reach its minimum value at blockage ratio β = 3 for all *Re* and then show a slight increase and decrease when the β increases (Fig. 6 (b)).

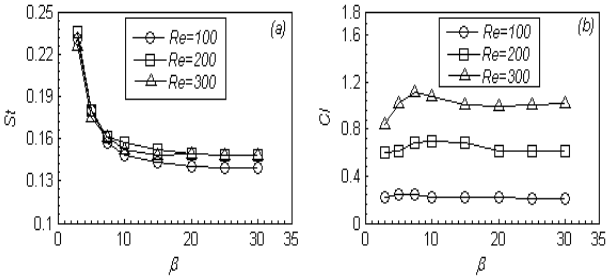

Fig. 6 (a) Strouhal number (b) peak value of the lift coefficient as a function of the blockage ratios for flow past the cylinder for fixed Reynolds number

Fig. 7 (a), shows that the *Cdrms* decreases with the increase of β and then almost remains constant for *Re* = 100 and 200. On the other hand, the same trend is observed for *Re* = 300 except for blockage ratio (β = 20) shows an abrupt change. It can be seen from Fig. 7 (b), that the *Clrms* initially increases and then shows a slight decrease and then almost remains constant for all *Re*.

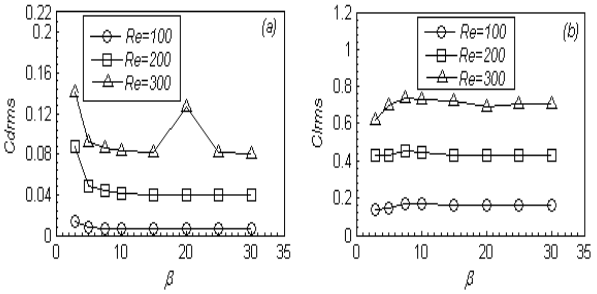

Fig. 7 (a) Root-mean-square value of the drag coefficient (b) root-mean-square value of the lift coefficient as a function of the blockage ratios for flow past the cylinder for fixed Reynolds number

The dependence of the *Cl*/*Cd* on β is clearly seen in Fig. 8. A slight increase of *Cl*/*Cd* has been observed for some β initially and then shows the constant, slight decrease and increase behavior as the β increases.

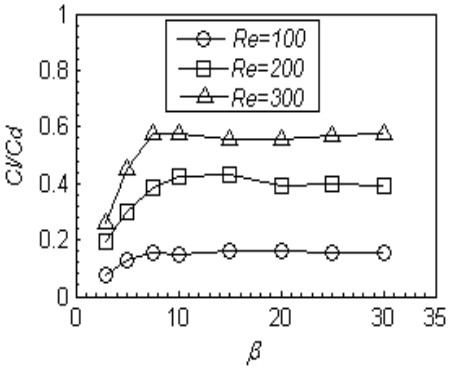

Fig. 8 The ratio between lift and drag coefficients as a function of the blockage ratios for flow past the cylinder for fixed Reynolds number

The present computational results show that when β increases from 3 to 20, *Cd*, <*Cd*> and *St* can be reduced by about 53.2%, 53.1%, and 39.3% at *Re* = 100, 48.9%, 48.5%, and 36.6% at *Re* = 200 and about 44.7%, 45.6%, and 34% at *Re* = 300, respectively. It is worth noticing that a remarkable reduction of such physical quantities occurs in the range $3 \leq \beta \leq 20$. When, $\beta > 20$, the reduction becomes insignificant.

A series of computations were carried out, by increasing the Reynolds number from 100 to 300 to determine the influence of *Re* for fixed blockage ratios. The *Cd*, <*Cd*>, *Cl*, *Cdrms*, *Clrms*, *Cl*/*Cd*, and *St* were computed and plotted for Reynolds number 100, 200, and 300 with fixed β.

The physical quantities such as *Cd* and <*Cd*> tend to increases as *Re* increases (Figs. 9 (a), (b)). This increase is consistent to the finding of other investigators such [7] for flow past a square cylinder. The increase in *Cd* being about 3.4% at β when Reynolds number increase from 100 to 200 and about 6.6% from Reynolds number 200 to 300 (Fig. 9 (a)). On the other hand, the increase in *Cd* at $\beta = 30$ is about 14.3% from Reynolds number 100 to 200 and about 14.6% from Reynolds number 200 to 300 (Fig. 9 (a)). These observations indicate that the side and width of the vortices becomes smaller at high blockage ratios and Reynolds number (see Figs. 2-4).

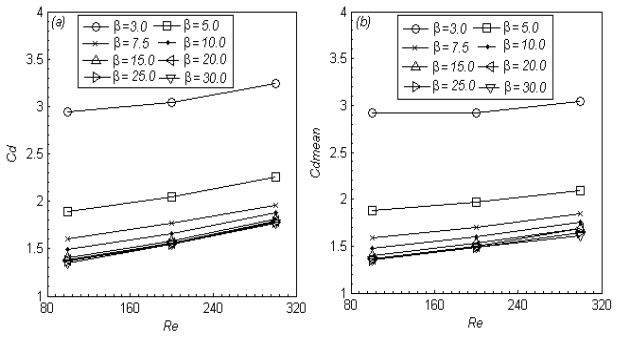

Fig. 9 Variation of physical quantities with Reynolds numbers: (a) drag coefficient; and (b) mean drag coefficient.

It can be seen from Fig. 10 (a) that the shedding frequency parameter Strouhal number increase for Reynolds number 200 and then shows a slight decrease for Reynolds number 300. This observation is consistent to the finding of [7] for flow past a square cylinder. The results show that unlike circular blockage, for square blockage, the *St* first increases and then decreases with an increase in *Re*. Fig. 10 (b) shows the variation of *Cl* versus *Re* for fixed blockage ratio. As shown in Fig. 10 (b), the *Cl* increases linearly with the *Re*.

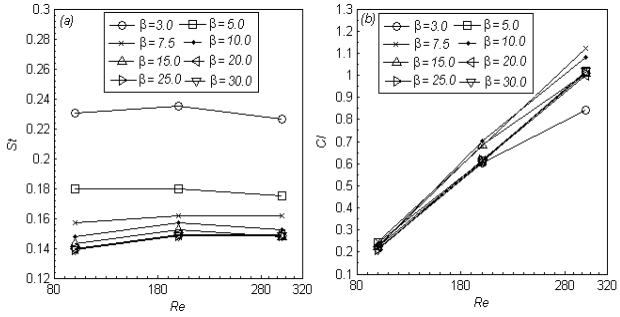

Fig. 10 Variation of physical quantities with Reynolds numbers: (a) Strouhal number; and (b) peak value of lift coefficient

A fairly stable value with slight increases of *Cdrms*, *Clrms*, and *Cl*/*Cd* has been observed for each β as the *Re* increases (Figs. 11 (a)-(c)). The above observations indicate that the strength of the vortex shedding depends on the *Re*. The higher the Reynolds numbers the stronger the vortex shedding. The blockage ratio effect on the vortex shedding is obviously stronger in high Reynolds number flows.

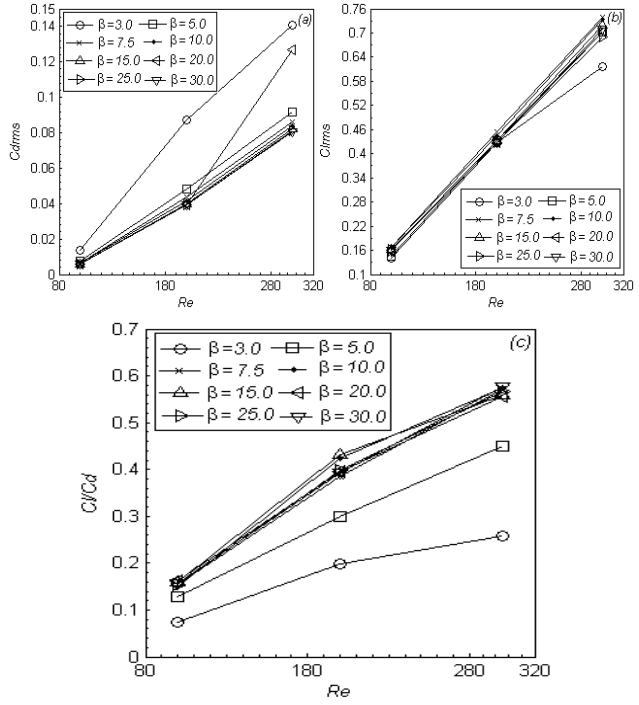

Fig. 11 Variation of physical quantities with Reynolds numbers: (a) root-mean-square value of the drag coefficient; (b) root-mean-square value of the lift coefficient; and (c) ratio between the lift and drag coefficients

It may be important to state here again that during the process of numerical simulations for β the lift and drag coefficients exhibit a regular periodic behavior; however, for the sake of brevity only two selected representative β = 3 and 30 cases will be discussed here. Figs. 12 (a)-(f) shows that *Cd* and *Cl* history developments for different β. It is noticed that the vortex shedding becomes periodic, and the frequency of the lift coefficient is twice that of the drag coefficient, which are consistent with those of [3] for all *Re*. The results show that *Cd* and *Cl* exhibit a regular periodic behavior for all chosen β and *Re*, as shown in Figs. 12 (a)-(f). These results show a periodic alternating vortex shedding corresponding to Figs. 2 and 4 because of regular periodic behavior of *Cd* and *Cl*.

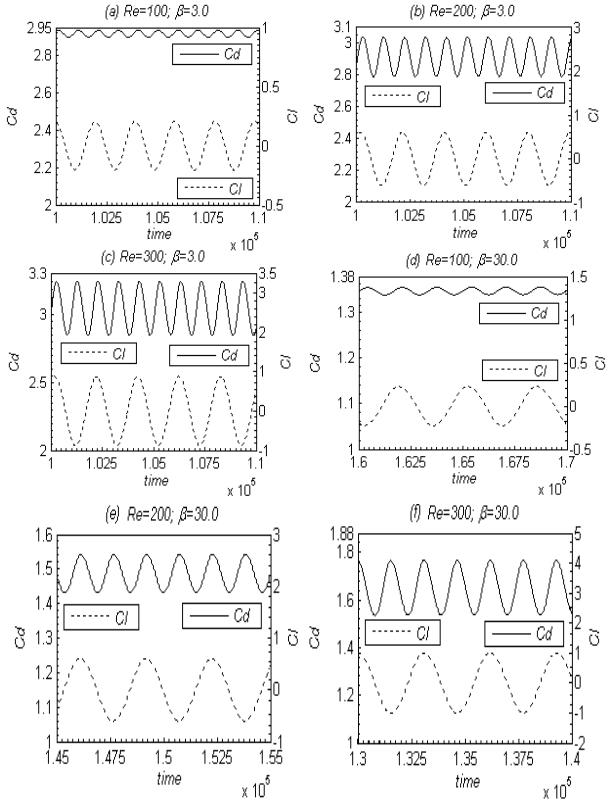

Fig. 12 Temporal evolution of lift and drag coefficients for flow past a square cylinder for Reynolds numbers 100, 200, 300 and two different values of blockage ratios β = 3 and 30

It can also be seen from Figs. 2 and 4 (a) that the vortices are cracked down and disappear in the far wake. This observation indicates the strong blockage effect. It can be seen from Figs. 12 (a)-(f) that the amplitudes of the fluctuating lift and drag coefficients grow as *Re* increase for fixed β.

Fourier analysis of the lift coefficients on the cylinders are carried out for all blockage ratios and Reynolds number. The Strouhal numbers obtained in the present work are shown in Figs. 13 (a)-(f) for two selected blockage ratios β = 3 and 30. The results show that there is only one wake behind the cylinder; the power spectra have only one peak frequency. This confirms the single-wake shedding mode at all blockage ratios.

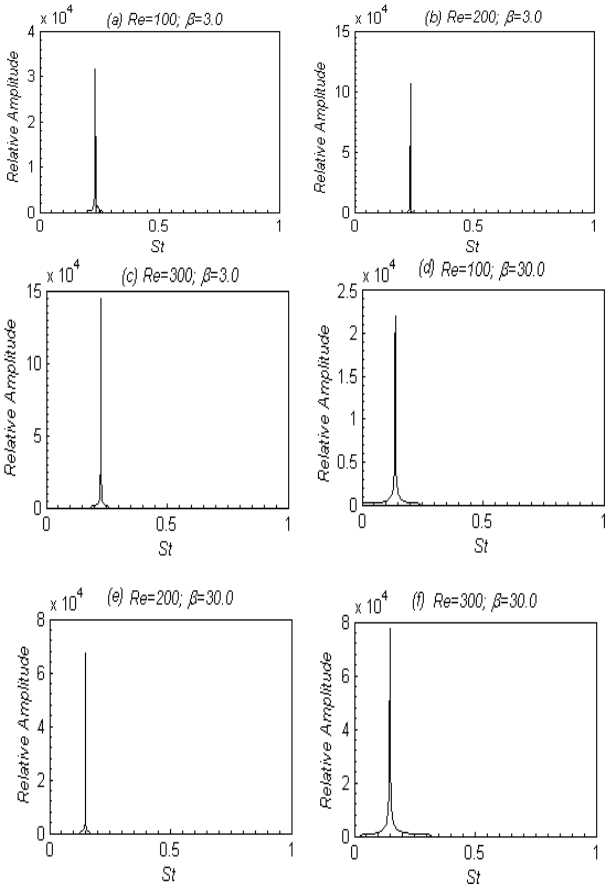

Fig. 13 Fourier spectra of lift force coefficient for Reynolds numbers 100, 200, 300 and four different values of blockage ratios β =3 and 30

In Figs. 14 (a)-(c), it can be seen that the computational time is not significantly affected when β increases from 3*d* to 30*d*. It is interesting to observe that the growth rate and the frequency of the perturbations are not affected significantly. Only a phase shift is observed as the blockage ratio is brought closer.

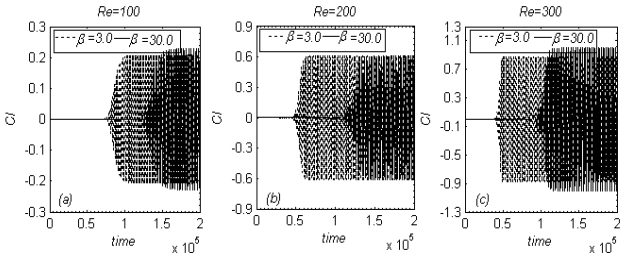

Fig. 14 Variation of the lift coefficient at = 100, 200 and 300 for two different blockage ratios (β = 3, 30)

In this section a comparison between flow past a row of circular and square cylinders with equispaced distance is

shown in Fig. 15. The variation of drag coefficient shows opposite trend for the flow past a square cylinder to that of a circular cylinder. In case of square cylinder the *Cd* increases continuously for *Re* at fixed blockage ratio. On the other hand, the *Cd* for the circular cylinder shows a decrease for *Re* at fixed blockage ratio.

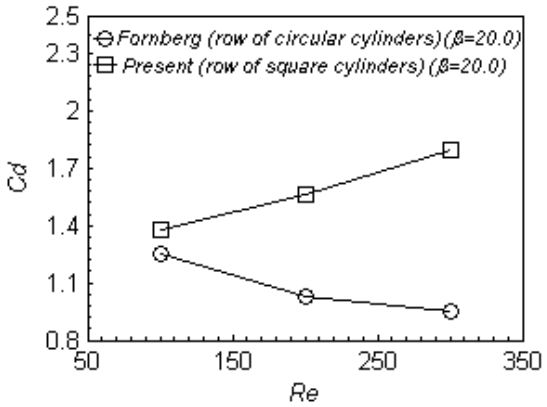

Fig. 15 Comparison between flow past a row of circular and square cylinders

The drag force is always lower for a circular cylinder than a square cylinder and this difference is due to higher bluffness related with square cylinder. This means that the flow separate much past in case of square cylinder because of the leading sharp edges.

V. Conclusions

Results are reported for a two-dimensional numerical investigation of the effect of equispaced distances between rows of square cylinders, for Reynolds number between 100 and 300, and blockage ratios ranging from 3 to 30 using the multi-relaxation-time lattice Boltzmann method. Symmetry boundary conditions have more blockage effect as compared to periodic boundary condition. The physical quantities such as drag and mean drag coefficients, and Strouhal numbers in general, decrease with increasing blockage ratios. All physical quantities such as drag and mean drag coefficients, peak value of the lift coefficient, and standard deviation value of the lift and drag coefficients linearly increase for each blockage ratio as the Reynolds number increases except Strouhal number. The results show that the drag and mean drag coefficients and the Strouhal number reach their maximum values at the blockage ratio (β = 3). We also found that the peak value of lift coefficient appears to reach its minimum value at blockage ratio β = 3 for all Reynolds number and then show a slight increase and decrease when the blockage ratios increases. We found that for unconfined flow the drag coefficient, mean drag coefficient and Strouhal number shows better results with the numerical data from open literature. We observed that increasing the blockage ratio from β = 20 to 30 have little effect on the physical quantities almost negligible. The computational cost is not significantly increase when the blockage ratios increased. We also found that the typical practical scenario is almost the same to [9] for the flow past a row of circular cylinders. On the basis of our analysis and conclusion the proposed MRT-LBM can be an effective guide to determine the flow visualization past a square cylinder in various computational cases.

References

[1] M. Cheng, and P. M. Moretti, "Experimental study of the flow field downstream of a single tube row," *Experimental Thermal Fluid Science*, vol.1, 1988, pp. 69-74.
[2] A. Okajima, "Strouhal numbers of rectangular cylinders," Journal of Fluid Mechanics, Cambridge, U.K. vol. 123, 1982, pp. 379-398.
[3] R. W. Davis, E. F. Moore, and L. P. Purtell, "A numerical experimental study of confined flow around rectangular cylinders," Physics of Fluids, Part A, vol. 27, 1984, pp. 46-59.
[4] R. Franke, W. Rodi, and B. Schonung, "Numerical calculation of Laminar Vortex Shedding flow past cylinders," Journal of Wind Engineering and Industrial Aerodynamics, vol. 35, 1990, pp. 237-257.
[5] A. Sohankar, L. Davidson, and C. Norberg, "Numerical simulation of unsteady flow around a square two-dimensional cylinder," Twelfth Australian Fluid Mechanics Conference, The University of Sydney, Australia. 1995, pp. 517-520.
[6] A. Sohankar, C. Norberg, and L. Davidson, "Simulation of three-dimensional flow around a square cylinder at moderate Reynolds numbers," Physics of Fluids. vol.11, 1999, pp. 288-306.
[7] A. K. Saha, K. Muralidhar, and G. Biswas, "Transition and Chaos in two-dimensional flow past a square cylinder," Journal of Engineering Mechanics, vol.126, 1999, pp. 523-532.
[8] D. B. Ingham, T. Tang, and B. R. Morton, "Steady two-dimensional flow through a row of normal flat plates," Journal of Fluid Mechanics, vol. 210, 1990, pp.281-302.
[9] B. Fornberg, "Steady incompressible flow past a row of circular cylinders," Journal of Fluid Mechanics, vol. 225, 1991, pp. 655-678.
[10] D. B. Ingham, and B. Yan, "Fluid flow around cascades," Zangew Mathematical Physics, vol. 44, 1993.
[11] R. Natarajan., B. Fornberg, and A. Acrivos, "Flow past a row of flat plates at large Reynolds numbers," Proceedings of Royal Society London A, vol. 441, 1993, pp. 211-235.
[12] S. R. Kumar., A. Sharma., and A. Agarwall, "Simulation of flow around a row of square cylinders," Journal of Fluid Mechanics, vol. 606, 2008, pp.369-397.
[13] S. U. Islam and C. Y. Zhou, "Numerical simulation of flow around a row of circular cylinders using the lattice Boltzmann method," Information Technology Journal, vol.8. , 2009, pp. 513-520.
[14] S. Ul. Islam, H. Rahman, and W. S. Abbasi, "Grid independence study of flow past a square cylinder using the multi-relaxation-time lattice Boltzmann method," International Journal of Mathematical, Computational, Physical and Quantum Engineering, World Academy of Science, Engineering and Technology, vol. 8, 2014, pp. 972-982.
[15] S. Ul. Islam, W. S. Abbasi, and H. Rahman, "Force statistics and wake structure mechanism of flow around a square cylinder at low Reynolds numbers," International Journal of Mechanical, Aerospace, Industrial and Mechatronics Engineering, vol. 8, 2014, pp. 1397-1403.
[16] Y. Dazchi, M. Renwei, L. S. Luo, and S. Wei, "Viscous flow computations with the method of lattice Boltzmann equation," Progress in Aerospace Sciences, vol. 39, 2003, pp. 329-367.